

## Oxetanes from [2+2] Cycloaddition of Stilbenes to Quinone via Photoinduced Electron Transfer†

Duoli Sun, Stephan M. Hubig, and Jay K. Kochi\*

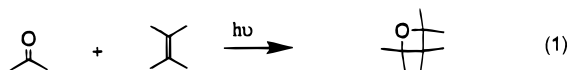
Department of Chemistry, University of Houston, Houston, Texas 77204-5641

Received August 26, 1998

The photochemical coupling of various stilbenes (**S**) and chloranil (**Q**) is effected by the specific charge-transfer (CT) activation of the precursor electron donor–acceptor (EDA) complex [**S**, **Q**], and the [2+2] cycloaddition is established by X-ray structure elucidation of the crystalline *trans*-oxetanes formed selectively in high yields. Time-resolved (fs/ps) spectroscopy reveals the (singlet) ion-radical pair  $^1[\text{S}^+, \text{Q}^-]$  to be the primary reaction intermediate and thus unambiguously establishes for the first time the electron-transfer pathway for this typical Paterno–Büchi transformation. The alternative cycloaddition via the specific activation of the carbonyl component (as a commonly applied procedure in Paterno–Büchi couplings) leads to the same oxetane regioisomers in identical molar ratios. As such, we conclude that a common electron-transfer mechanism applies via the quenching of the photoactivated quinone acceptor by the stilbene donor to afford triplet ion-radical pairs  $^3[\text{S}^+, \text{Q}^-]$  which appear on the ns/ $\mu\text{s}$  time scale. The spin multiplicities of the critical ion-pair intermediate [**S**<sup>+</sup>, **Q**<sup>−</sup>] in the two photoactivation methodologies determine the time scale of the reaction sequences (which are otherwise the same), and thus the efficiency of the relatively slow ion-pair collapses ( $k_c \cong 10^8 \text{ s}^{-1}$ ) to the 1,4-biradical that ultimately leads to the oxetane product.

### Introduction

The photoinduced [2+2] cycloaddition of an olefin to a carbonyl center, also known as the Paterno–Büchi reaction,<sup>1</sup> is a synthetically useful photochemical transformation since it provides a simple route to the preparation of oxetanes with high regio- and stereoselectivity (eq 1).<sup>2</sup>



The scope of this photocycloaddition has been widely expanded over the years to include (a) the preparation of diastereochemically pure oxetanes<sup>3</sup> and oxetane-containing natural products,<sup>4,5</sup> and (b) spectroscopic studies<sup>6</sup> leading to the discovery of various reactive intermediates including exciplexes,<sup>7–9</sup> ion-radical pairs,<sup>9–13</sup> and 1,4-biradicals.<sup>2,11–14</sup> However, the temporal sequence

and the mechanistic relevance of the transient species have not been established in most studies, and the general validity of an electron-transfer mechanism is controversial. In fact, there is still no definitive answer to the question as to whether (a) the 1,4-biradicals that are observed in Paterno–Büchi couplings<sup>11–14</sup> result *directly* from the quenching of photoexcited carbonyl by the olefin, or whether (b) other reactive intermediates (such as exciplexes<sup>7–9</sup> or ion-radicals<sup>9–13</sup>) represent the initial quenching products that are *subsequently* converted to biradicals. These ambiguities in the identification of the primary reactive intermediates are inherent to the photoactivation methodology that is commonly applied in Paterno–Büchi couplings. Thus, the photoexcitation of the carbonyl leads to its excited (singlet or triplet) state which is known to be quenched via a variety of pathways, including energy transfer, electron transfer, bond formation, bond cleavage, etc. As a result, different reactive species may be observed initially, but the primary quenching product cannot be unambiguously identified (experimentally) since the observation and identification depend critically on its lifetime and spectroscopic accessibility.

† Dedicated to Professor George H. Büchi (Aug 1, 1921 to Aug 28, 1998) in memoriam.

(1) (a) Paterno, E.; Chieffi, G. *Gazz. Chim. Ital.* **1909**, *39*, 341. (b) Büchi, G.; Inman, C. G.; Lipinsky, E. S. *J. Am. Chem. Soc.* **1954**, *76*, 4327.

(2) For reviews, see: (a) Demuth, M.; Mikail, G. *Synthesis* **1989**, 145. (b) Porco, J. A.; Schreiber, S. L. In *Comprehensive Organic Synthesis*; Trost, B. M., Fleming, I., Paquette, L. A., Eds.; Pergamon: New York, 1991; Vol. 5, p 151. (c) Griesbeck, A. G. In *CRC Handbook of Organic Photochemistry and Photobiology*; Horspool, W. M., Song, P.-S., Eds.; CRC Press: Boca Raton, FL, 1995; p 522. (d) Arnold, D. R. *Adv. Photochem.* **1968**, *6*, 301. (e) Creed, D. In ref 2c, p 737ff. (f) Jones, G., II. In *Organic Photochemistry*; Padwa, A., Ed.; Dekker: New York, 1981; Vol. 5, p 1.

(3) (a) Bach, T.; Jödicke, K.; Kather, K.; Fröhlich, R. *J. Am. Chem. Soc.* **1997**, *119*, 2437. (b) Bach, T.; Eilers, F.; Kather, K. *Liebigs Ann. Recl.* **1997**, 1529. (c) Bach, T. *Liebigs Ann. Recl.* **1997**, 1627. (d) Bach, T.; Schröder, J. *Tetrahedron Lett.* **1997**, 3701.

(4) (a) Mattay, J.; Buchkremer, K. *Helv. Chim. Acta* **1988**, *71*, 981. (b) Mattay, J.; Buchkremer, K. *Heterocycles* **1988**, *27*, 2153.

(5) (a) Schreiber, S. L. *J. Am. Chem. Soc.* **1983**, *105*, 660. (b) Schreiber, S. L.; Satake, K. *J. Am. Chem. Soc.* **1984**, *106*, 4186.

(6) For a review that emphasizes the mechanistic considerations, see ref 2f.

(7) (a) Caldwell, R. A.; Hrcncir, D. C.; Muñoz, T., Jr.; Unett, D. J. *J. Am. Chem. Soc.* **1996**, *118*, 8741. (b) Caldwell, R. A.; Sovocool, G. W.; Gajewski, R. P. *J. Am. Chem. Soc.* **1973**, *95*, 2549.

(8) Schore, N. E.; Turro, N. J. *J. Am. Chem. Soc.* **1975**, *97*, 2482.

(9) Hu, S.; Neckers, D. C. *J. Org. Chem.* **1997**, *62*, 6820.

(10) Gersdorf, J.; Mattay, J.; Görner, H. *J. Am. Chem. Soc.* **1987**, *109*, 1203.

(11) (a) Freilich, S. C.; Peters, K. S. *J. Am. Chem. Soc.* **1985**, *107*, 3819. (b) Freilich, S. C.; Peters, K. S. *J. Am. Chem. Soc.* **1981**, *103*, 6255.

(12) Griesbeck, A. G.; Mauder, H.; Stadtmüller, S. *Acc. Chem. Res.* **1994**, *27*, 70.

(13) Eckert, G.; Goetz, M. *J. Am. Chem. Soc.* **1994**, *116*, 11999.

(14) (a) Schuster, D. I.; Lem, G.; Kaprinidis, N. A. *Chem. Rev.* (Washington, D.C.) **1993**, *93*, 3. (b) Hu, S.-H.; Neckers, D. C. *J. Org. Chem.* **1997**, *62*, 564.

Chart 1

	1	2	3	4	5	6	7	8
$E^P_{ox}$ [V vs. SCE]	1.56	1.59	1.71	1.44	1.46	1.58	1.58	1.83

To circumvent these mechanistic ambiguities which are inherent to carbonyl-activated photocouplings, we now take a different approach to explore the viability of an initial electron transfer in Paterno–Büchi reactions. Thus, the charge-transfer (CT) activation of the electron donor–acceptor (EDA) complex<sup>15,16</sup> between carbonyls and olefins represents the unambiguous method for generating ion-radical pairs spontaneously and exclusively as the primary reaction intermediates.<sup>17</sup> As such, we will demonstrate that the ion-radical pair is the common precursor of the final (oxetane) products and any other reactive (biradical) intermediate. To this end, we choose the stilbenes (**S**) in Chart 1 as prototypical olefinic donors and chloranil (**Q**) as the carbonyl acceptor, since both components are readily involved in the rapid pre-equilibrium formation of intermolecular EDA complexes, i.e.,<sup>18</sup>



In each case, the CT absorption bands can be selectively irradiated at wavelengths  $\lambda_{exc} > 480 \text{ nm}$ <sup>19</sup> (where neither chloranil nor the stilbenes absorb).

Accordingly, our first task in this study is (a) to show that the specific CT excitation of the EDA complex in eq 2 is a viable photochemical procedure and (b) to establish the nature of the [2+2] cycloaddition by isolation and X-ray crystallographic analysis of the crystalline *trans*-oxetane photoadducts. Since stilbene cation radical<sup>20</sup> and chloranil anion radical<sup>21</sup> both exhibit diagnostic absorption bands in the UV–vis wavelength region, we exploit time-resolved (ps) spectroscopy to identify the singlet ion-radical pair<sup>22</sup>  $^1[S^+, Q^-]$  as the primary reactive intermediate upon photoexcitation of the chloranil/stilbene EDA complex, i.e.,



(15) Foster, R. *Organic Charge-Transfer Complexes*; Academic Press: New York, 1969.

(16) (a) Briegleb, G. *Elektronen Donator-Acceptor Komplexe*; Springer: Berlin, 1961. (b) Andrew, L. J.; Keefer, R. M. *Molecular Complexes in Organic Chemistry*; Holden-Day: San Francisco, 1964.

(17) Charge-transfer excitation of EDA complexes effects the transfer of an electron from the donor to the acceptor in less than 500 fs. See: Wynne, K.; Galli, C.; Hochstrasser, R. M. *J. Chem. Phys.* **1994**, *100*, 4797.

(18) See ref 15, p 40.

(19) The CT absorption band of the stilbene/chloranil EDA complex is centered at 510 nm. See ref 18.

(20) (a) Lewis, F. D.; Bedell, A. M.; Dykstra, R. E.; Elbert, J. E.; Gould, I. R.; Farid, S. *J. Am. Chem. Soc.* **1990**, *112*, 8055. (b) Jungmann, H.; Gusten, H.; Schulte-Frohlinde, D. *Chem. Rev.* **1968**, *68*, 2690. (c) Shida, T. *Electronic Absorption Spectra of Radical Ions*; Elsevier: New York, 1988.

The subsequent (dark) coupling of this ion-radical pair to the 1,4-biradical is then the critical first step toward oxetane formation.<sup>23</sup> Such an unambiguous demonstration of oxetane formation by photoinduced electron transfer will then be related to the Paterno–Büchi cycloaddition—as usually carried out by specific carbonyl activation<sup>24</sup>—via the detailed comparison of (a) the oxetane-product mixtures and (b) the ion-pair kinetics for charge-transfer versus carbonyl activation.<sup>25</sup>

## Results and Discussion

**I. Oxetane Formation via Charge-Transfer Activation of the Stilbene/Quinone EDA Complex.** Vivid colors appeared immediately upon the addition of (*E*)-stilbene (**S**) to chloranil (**Q**) owing to the spontaneous formation of the intermolecular EDA complex [**S**, **Q**] in eq 2.<sup>18</sup> [Note the EDA complex exhibited the characteristic (charge-transfer) absorption bands in a wavelength region where neither chloranil nor the stilbenes absorb (see Figure 1.)] Similar spectral changes were observed with the other (substituted) stilbenes in Chart 1, and the formation constants  $K_{EDA}$  and the extinction coefficients  $\epsilon_{CT}$  of the EDA complexes in Table 1 were evaluated by the quantitative analysis of the spectral data according to the Benesi–Hildebrand treatment<sup>29</sup> (see the Experimental Section).

Specific excitation of the charge-transfer absorption bands (see Table 1) of the chloranil complexes with

(21) André, J. J.; Weill, G. *Mol. Phys.* **1968**, *15*, 97.

(22) Ojima, S.; Miyasaka, H.; Mataga, N. *J. Phys. Chem.* **1990**, *94*, 4147.

(23) (a) According to the electron-transfer mechanism for the Paterno–Büchi photocyclization, the initial photoinduced electron transfer to afford the ion-radical pair is followed by a fast (dark) reaction involving ion-pair collapse to the 1,4-biradical and subsequent ring closure, i.e.,



(b) For the observation of 1,4-biradicals from the related benzoquinone and styrene, see: (c) Maruyama, K.; Otsuki, T.; Tai, S. *J. Org. Chem.* **1985**, *50*, 52. (d) Maruyama, K.; Imahori, H. *J. Org. Chem.* **1989**, *54*, 2693.

(24) Xu, J.-H.; Wang, L.-C.; Xu, J.-W.; Yan, B.-Z.; Yuan, H.-C. *J. Chem. Soc., Perkin Trans. 1* **1994**, 571.

(25) In this regard, the present study draws upon our earlier investigation of the photoinduced coupling of a series of diphenylacetylene donors with 2,6-dichlorobenzoquinone, also designated as a Paterno–Büchi coupling,<sup>26</sup> although the putative (highly unstable) oxetenes<sup>28</sup> were merely inferred as intermediates<sup>27</sup> (direct observation notwithstanding). Accordingly, we focus here on stilbene donors more closely akin to the original Paterno–Büchi substrates from which we could actually isolate the [2+2] cycloadducts and verify their oxetane structures by X-ray crystallography.

(26) Bosch, E.; Hubig, S. M.; Kochi, J. K. *J. Am. Chem. Soc.* **1998**, *120*, 386.

(27) (a) Barltrop, J. A.; Hesp, B. *J. Chem. Soc. (C)* **1967**, 1625. (b) Farid, S.; Kothe, W.; Pfundt, G. *Tetrahedron Lett.* **1968**, 4147. (c) Pappas, S. P.; Portnoy, N. A. *J. Org. Chem.* **1968**, *33*, 2200.

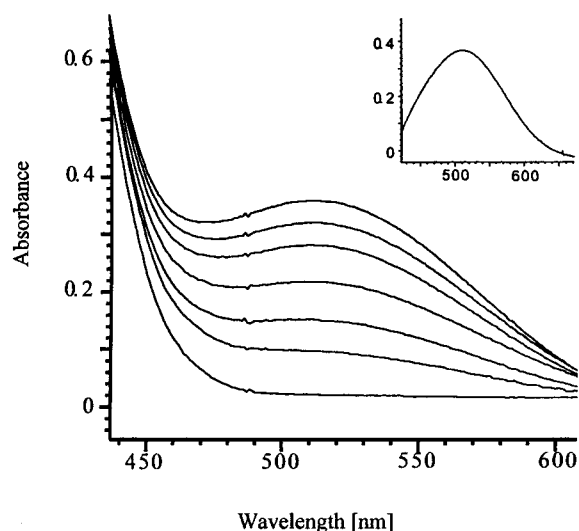
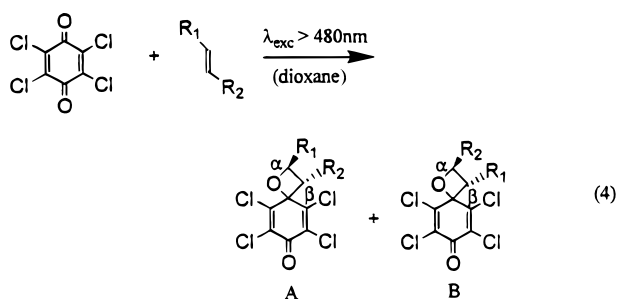


**Figure 1.** UV-vis spectral changes upon the incremental addition of stilbene to a benzene solution of 0.005 M chloranil at  $[S] = 0, 0.024, 0.032, 0.043, 0.051, 0.071,$  and  $0.081$  M (bottom-to-top). Inset: Charge-transfer spectrum of the  $[S, Q]$  complex by digital subtraction of chloranil.

various stilbenes was achieved by irradiation at wavelengths  $\lambda_{exc} > 480$  nm where neither uncomplexed chloranil nor the stilbenes absorbed. For example, an equimolar solution of chloranil and (*E*)-stilbene (**1**) in dioxane was exposed to visible light for an extended period of time. Periodic HPLC analysis of the photolyzate revealed the simultaneous disappearance of (*E*)-stilbene and chloranil and the monotonic appearance of a single product which was identified as the spirooxetane **1A** in Table 2. Charge-transfer activation of chloranil complexes with the other stilbenes in Chart 1 yielded a pair of isomeric oxetane products **A** and **B** described in eq 4 (where  $R_1$  and  $R_2$  represented substituted phenyl groups), *i.e.*,



Symmetrical stilbenes ( $R_1 = R_2$ ) stereoselectively afforded a single spirooxetane isomer. Unsymmetrical stilbenes generated only two (out of four) possible stereoisomers (see eq 4), and the isomer ratios for the oxetane products are reported in Table 2. In no case were other isomeric adducts (such as cyclobutanes) found.<sup>30</sup> X-ray crystallographic analysis of the single crystals of **2A**, **3B**, and **6B** established the *trans*-configuration of the oxetane products, as illustrated in Figure 2, and the *trans*-configuration was also assigned to the other oxetane

**Table 1.** CT Absorption Maxima ( $\lambda_{CT}$ ), Formation Constants ( $K_{EDA}$ ), and Extinction Coefficients ( $\epsilon_{CT}$ ) of the EDA Complexes of Chloranil and Stilbene Donors<sup>a</sup>

stilbene donor	$E_{ox}^p$ [V vs SCE]	$\lambda_{CT}$ [nm]	$K_{EDA}$ [ $M^{-1}$ ]	$\epsilon_{CT}$ [ $M^{-1} \text{cm}^{-1}$ ]
<b>2</b>	1.59 <sup>b</sup>	507	1.1	592
<b>1</b>	1.56 <sup>b</sup>	510	1.6	680
<b>5</b>	1.46 <sup>c</sup>	533	2.6	286
<b>4</b>	1.44 <sup>b</sup>	540	3.1	189

<sup>a</sup> In benzene solution at 23 °C. <sup>b</sup> Oxidation (peak) potentials taken from ref 20a and converted by subtracting 0.39 V from the values vs Ag/AgI. <sup>c</sup> Determined by cyclic voltammetry.

**Table 2.** Charge-Transfer-Activated[2+2] Coupling of Stilbenes with Chloranil<sup>a</sup>

Stilbene Donor <sup>b</sup>	Oxetane Products (yield, %) <sup>c</sup>
<b>1</b>	<b>1A</b> (99)
<b>2</b>	<b>2A</b> (44) <b>2B</b> (55)
<b>3</b>	<b>3A</b> (45) <b>3B</b> (55)
<b>4</b>	<b>4A</b> <sup>d</sup> <b>4B</b> <sup>d</sup>
<b>5</b>	<b>5A</b> <sup>d</sup> <b>5B</b> <sup>d</sup>
<b>6</b>	<b>6A</b> (40) <b>6B</b> (60)
<b>7</b>	<b>7A</b> (100)
<b>8</b>	<b>8A</b> (98)

<sup>a</sup> In dioxane solution containing 0.05 M chloranil and 0.1 M stilbene under argon at 25 °C irradiation at  $\lambda_{exc} > 480$  nm. <sup>b</sup> Identified in Chart 1. <sup>c</sup> At ca. 2–5% conversion achieved after ca. 50 h irradiation. <sup>d</sup> Oxetane isomers obtained only by carbonyl activation (see Experimental Section).

isomers (**4**, **5**, **7**, and **8**) in Table 2. No (HPLC) evidence for the formation of *cis*-isomers was found. The regiochemistry of the coupling resulting in the isomers **A** and **B** in Table 2 was determined by <sup>1</sup>H NMR analysis (see the Experimental Section).<sup>31</sup> Thus, the photocoupling of chloranil with various substituted stilbenes always resulted in the formation of oxetanes with high (*trans*)

(28) Oxetenes are short-lived and exhibit lifetimes of up to several hours only at low temperatures. See: (a) Friedrich, L. E.; Bower, J. D. *J. Am. Chem. Soc.* **1973**, *95*, 6869. (b) Friedrich, L. E.; Lam, P.-S. *J. Org. Chem.* **1981**, *46*, 306. (c) Friedrich, L. E.; Schuster, G. B. *J. Am. Chem. Soc.* **1971**, *93*, 4602.

(29) (a) Benesi, H.; Hildebrand, J. H. *J. Am. Chem. Soc.* **1949**, *71*, 2703. (b) Person W. B. *J. Am. Chem. Soc.* **1965**, *87*, 167.

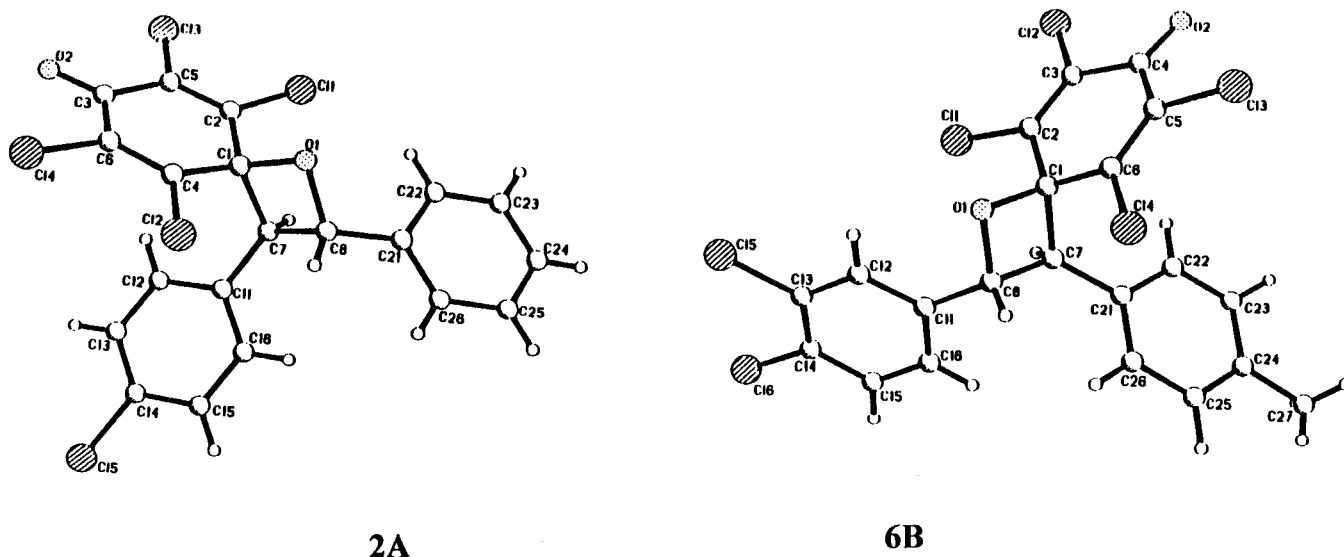


**Figure 2.** PLUTO perspective of spirooxetanes **2A** and **6B** showing the *trans*-configuration and regiochemistry of the cycloadducts.

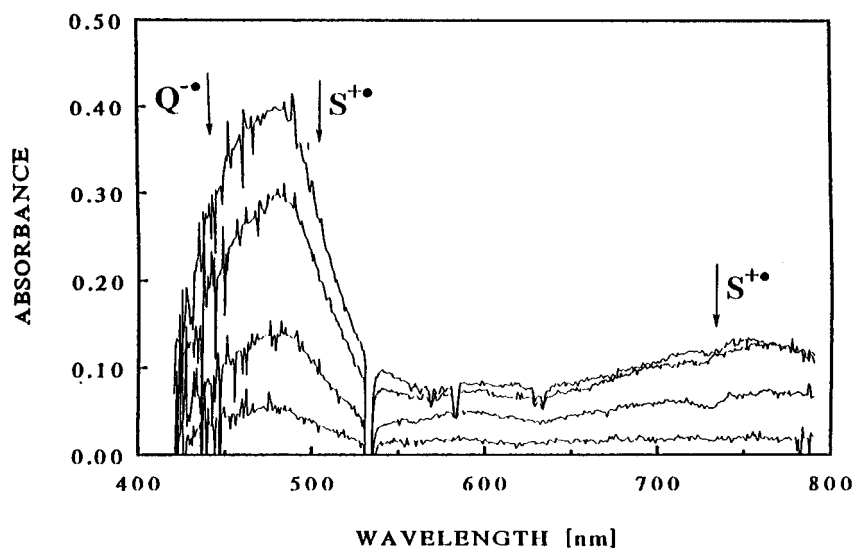


**Figure 3.** Transient spectrum obtained at 30, 40, 50, and 80 ps (top-to-bottom) upon the application of a 25 ps laser pulse at  $\lambda_{CT} = 532$  nm to a solution of 0.6 M stilbene and 0.005 M chloranil in dioxane.

stereoselectivity, but indifferent regioselectivity. However, regardless of the detailed selectivity, the important result from the above-described photochemical experiments is the fact that the Paterno–Büchi coupling of various stilbenes with quinone can be successfully achieved by the specific charge-transfer excitation of their intermolecular EDA complexes to yield exclusively<sup>30</sup> oxetane adducts that are structurally verified by X-ray crystallography.

## II. Direct Observation of the Ion-Radical Pair [ $S^+$ , $Q^{\cdot-}$ ] as the Primary Intermediate in the Charge-

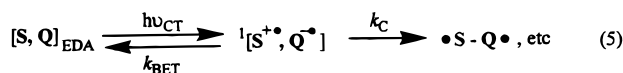
(30) (a) By contrast, C–C cycloadditions of photoactivated quinones (leading to cyclobutane products) are observed with arylethenes such as styrenes and 1,1-diphenylethenes,<sup>30b</sup> and in photocycloadditions of either stilbene to the parent benzoquinone<sup>30c</sup> or phenylacetylenes to methoxy-substituted quinones.<sup>30d</sup> (b) Covell, C.; Gilbert, A.; Richter, C. *J. Chem. Res. (S)* **1998**, 316. (c) Gilbert, A.; Kamonnawin, P. Unpublished results (reported in ref 30b). (d) Pappas, S. P.; Pappas, B. C.; Portnoy, N. A. *J. Org. Chem.* **1969**, *34*, 520.

(31) The regiochemistry of the coupling could not be established by GC/MS analysis owing to complete decomposition of the spirooxetanes (to the starting materials) upon their injection into the gas chromatograph.

**Transfer Activation of Chloranil/Stilbene Complexes.** The successful preparation of oxetane adducts by CT activation of chloranil/stilbene complexes necessitated our next task to identify the primary reaction intermediate in this photocoupling process. Accordingly, the (ground-state) EDA complex of chloranil and stilbene (**1**) was selectively excited by the deliberate irradiation of its charge-transfer absorption band in Figure 1 with the 25 ps laser pulse at 532 nm (from a mode-locked Nd:YAG laser). First, a solution of chloranil (0.005 M) and (*E*)-stilbene (0.6 M) in dioxane was exposed to the 532 nm laser pulse, and the resulting time-resolved (ps) absorption spectra are shown in Figure 3. The principal spectral feature that was immediately apparent upon the laser excitation consisted of a strong absorption band at  $\lambda_{max} = 480$  nm and a weak, broad band around 760 nm, which coincided with the composite absorptions of the chloranil anion radical ( $Q^{\cdot-}$ )<sup>21</sup> and the (*E*)-stilbene cation radical ( $S^+$ ).<sup>20</sup> In other words, both ion radicals ( $Q^{\cdot-}$ ) and ( $S^+$ ) were generated spontaneously within the 25 ps laser-pulse duration as depicted in eq 3. Subsequently,



Scheme 1



the quinone and the stilbene absorption bands decayed simultaneously within the 25 ps pulse with decay rate constants of  $k \geq 4 \times 10^{10} \text{ s}^{-1}$  (see Figure 3). Similar time-resolved (ps) absorption spectra were obtained in acetonitrile and benzene solution and also upon 532 nm excitation of the chloranil complexes with the other (substituted) stilbenes. In all cases, the decay rate constants exceeded  $k > 4 \times 10^{10} \text{ s}^{-1}$ , which corresponded to the time resolution of the 25 ps laser spectrometer. The chloranil/stilbene complex was also irradiated with the 200 fs laser pulse at 406 nm of a Ti:sapphire laser to obtain a more accurate rate constant for the ultrafast decay of the ion radicals. Despite the fact that at  $\lambda_{\text{exc}} = 406 \text{ nm}$  chloranil also absorbed the laser light to some extent, we clearly observed initially a strong transient absorption band at  $\lambda_{\text{max}} = 480 \text{ nm}$  with a shoulder at 450 nm which was readily ascribed to the stilbene cation radical and the chloranil anion radical, respectively. This initial transient spectrum subsequently decayed on the early picosecond time scale, and a first-order decay rate constant of  $k = 3 \times 10^{11} \text{ s}^{-1}$  was determined from the exponential fit of the absorbance/time profile.

The ultrafast generation and decay of the chloranil anion radical and the stilbene cation radical upon laser excitation is in accord with Mulliken theory, which predicts a spontaneous and complete electron transfer from the stilbene donor to the quinone acceptor upon CT excitation of their mutual EDA complex.<sup>32</sup> As a result, a *singlet* ion-radical pair  ${}^1[S^{\bullet+}, Q^{\bullet-}]$  is formed<sup>22</sup> (see Figure 3) which is identified by its ultrashort ( $\tau \cong 3 \text{ ps}$ ) lifetime. *This very first intermediate is formed exclusively in the photoexcitation of the EDA complex, and it is therefore the precursor to the oxetane coupling products in Table 2* (which are preparatively obtained by essentially the same irradiation method). In other words, the successful preparation of the oxetane coupling products by charge-transfer activation of the chloranil/stilbene complexes combined with the unambiguous identification of ion-radical pairs as the primary reactive intermediates provides direct (irrefutable) evidence for our conclusion that this typical Paterno–Büchi coupling of chloranil and stilbene occurs via an initial electron-transfer step. The ion-radical pair is thus the critical intermediate which undergoes the coupling ultimately to the oxetane product via the formation of an intermediate 1,4-biradical.<sup>23</sup> However, besides the coupling step ( $k_{\text{C}}$ ) the singlet ion pair can also undergo back electron transfer<sup>33</sup> ( $k_{\text{BET}}$ ) to restore the original EDA complex (Scheme 1).

In fact, the latter pathway is known to be very efficient in singlet ion-radical pairs,<sup>33</sup> and thus the competition between rapid back electron transfer and coupling in Scheme 1 will limit the quantum efficiency of oxetane formation significantly, as reported in the following section.

**III. Quantum Efficiencies for the Charge-Transfer-Activated Oxetane Formation.** The quantum yields

(32) (a) Mulliken, R. S. *J. Am. Chem. Soc.* **1950**, *72*, 600. (b) Mulliken, R. S. *J. Am. Chem. Soc.* **1952**, *74*, 811.

(33) (a) Asahi, T.; Mataga, N. *J. Phys. Chem.* **1989**, *93*, 6575. (b) Asahi, T.; Mataga, N. *J. Phys. Chem.* **1991**, *95*, 1956. (c) Peters, K. S. *Adv. Electron-transfer Chem.* **1994**, *4*, 27. (d) Hilinski, E. F.; Masnovi, J. M.; Kochi, J. K.; Rentzepis, P. M. *J. Am. Chem. Soc.* **1984**, *106*, 8071. (e) Fox, M. A. *Adv. Photochem.* **1986**, *13*, 237.29.

for oxetane formation via CT activation were determined using the 546 nm output of a mercury lamp as the irradiation source and a potassium reineckate solution<sup>34</sup> as the actinometer (see the Experimental Section). Although the resulting quantum efficiencies listed in Table 3 show that the photocoupling of chloranil and stilbene by CT activation is rather inefficient, there is a clear trend in  $\Phi_{\text{CT}}$  with the substitution pattern of the stilbene, the highest yield ( $\Phi_{\text{CT}} = 0.0012$ ) being achieved with the 4,4'-dichloro-substituted stilbene (**7**, see Table 3).

The low quantum efficiencies ( $\Phi_{\text{CT}}$ ) of oxetane formation can be traced to a highly efficient back electron transfer of the singlet ion-radical pair in Scheme 1.<sup>33</sup> If this pathway occurs with rate constants that are orders of magnitude faster than the coupling, the changes in the quantum yields  $\Phi_{\text{CT}}$  in Table 3 can be ascribed to variations in back electron transfer as predicted by Marcus theory for donors with different oxidation potentials<sup>35</sup> in Scheme 1.

According to Scheme 1, the efficiency ( $\Phi_{\text{CT}}$ ) of oxetane formation is a direct measure of the competition between coupling ( $k_{\text{C}}$ ) and back electron transfer ( $k_{\text{BET}}$ ), *i.e.*,  $\Phi_{\text{CT}} = k_{\text{C}}/(k_{\text{C}} + k_{\text{BET}})$ . Accordingly, by taking  $\Phi_{\text{CT}} = 3 \times 10^{-4}$  (from Table 3) and  $(k_{\text{C}} + k_{\text{BET}}) = 3 \times 10^{11} \text{ s}^{-1}$  (vide supra), we calculate the rate constant of coupling between  $Q^{\bullet-}$  and  $S^{\bullet+}$  within the singlet ion-radical pair to be  $k_{\text{C}} \cong 9 \times 10^7 \text{ s}^{-1}$  (in dioxane). In other words, the low quantum efficiencies for oxetane formation via CT activation of the chloranil/stilbene EDA complexes are the direct result of a very rapid back electron transfer ( $k_{\text{BET}} \cong 3 \times 10^{11} \text{ s}^{-1}$ ), which is known to be characteristic for singlet ion-radical pairs.<sup>33</sup> Thus, the CT activation methodology introduced in this study successfully establishes the viability of the electron-transfer pathway for the [2+2] cycloaddition of chloranil with stilbene. However, it is not a synthetically relevant procedure (owing to its low quantum efficiency), and we now turn to the commonly applied irradiation methodology for Paterno–Büchi reactions and focus on the results of oxetane formation by carbonyl (quinone) activation.

**IV. Oxetane Formation via Carbonyl (Quinone) Activation.** Selective photoactivation of the chloranil was achieved by irradiation at wavelengths  $\lambda_{\text{exc}} > 370 \text{ nm}$  where the stilbenes do not absorb.<sup>36</sup> For example, an equimolar (0.1 M) solution of (*E*)-stilbene (**1**) and chloranil was irradiated in dioxane until periodic HPLC analysis revealed the complete consumption of the chloranil. Oxetane **1A** was isolated as the single photoproduct and shown to be identical to that obtained by charge-transfer activation of the corresponding EDA complex (vide supra). Most importantly, the carbonyl-activated cycloadditions of the other (substituted) stilbenes in Chart 1 consistently led to the same isomeric oxetanes

(34) Wegner, E. E.; Adamson, A. W. *J. Am. Chem. Soc.* **1966**, *88*, 394. See also: Bunce, N. J. In *Handbook of Organic Photochemistry*; Scaiano, J. C., Ed.; Vol. 1: Chapter 9, p 241.

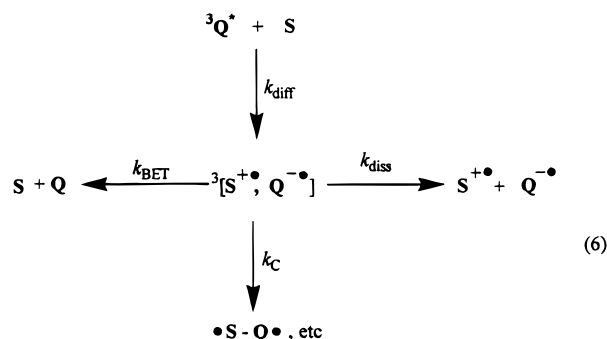
(35) With increasing oxidation potentials of the stilbene, the back electron transfer from stilbene cation radical to chloranil anion radical becomes more exergonic, and thus its rate constant will decrease in the Marcus-inverted region. See: (a) Marcus, R. A. *Annu. Rev. Phys. Chem.* **1964**, *15*, 155. (b) Marcus, R. A. *J. Chem. Phys.* **1965**, *43*, 679. (c) Marcus, R. A. *Faraday Discuss. Chem. Soc.* **1982**, *74*, 7. (d) Marcus, R. A. *J. Chem. Phys.* **1956**, *24*, 966.

(36) Note that at these concentrations, the absorption of actinic light by the chloranil/stilbene complex was negligible compared to that of the chloranil component owing to the limited values of  $K_{\text{EDA}}$  and  $\epsilon_{\text{CT}}$  in Table 1.

**Table 3. Comparison of CT-Activated and Carbonyl-Activated Photocoupling of Stilbenes with Chloranil**

stilbene donor	oxetane	CT activation <sup>a</sup> ratio <sup>c</sup> (A:B)	$\Phi_{CT}^d$ [ $\pm 0.0001$ ]	oxetane	carbonyl activation <sup>b</sup> ratio <sup>c</sup> (A:B)	$\Phi_Q^e$ [ $\pm 0.01$ ]
<b>1</b>	<b>1A</b>		0.0003	<b>1A</b>		0.34
<b>2</b>	<b>2A, 2B</b>	45:55	0.0005	<b>2A, 2B</b>	46:54	0.35
<b>3</b>	<b>3A, 3B</b>	45:55	0.0007	<b>3A, 3B</b>	47:53	0.33
<b>4</b>		no reaction		<b>4A, 4B</b>	40:60	0.03
<b>5</b>		no reaction		<b>5A, 5B</b>	46:54	0.11
<b>6</b>	<b>6A, 6B</b>	40:60	0.0004	<b>6A, 6B</b>	41:59	0.29
<b>7</b>	<b>7A</b>		0.0012	<b>7A</b>		0.48
<b>8</b>	<b>8A</b>		0.0011	<b>8A</b>		0.34

<sup>a</sup> Solution of 0.05 M chloranil and 0.1 M (*E*)-stilbene in dioxane irradiated at  $\lambda_{exc} = 546$  nm or  $\lambda_{exc} = 436$  nm. <sup>b</sup> The composition of the photolysate analyzed by HPLC with biphenyl as an internal standard. <sup>c</sup> Quantum yield by Reineckate salt actinometry. <sup>d</sup> Quantum yield by ferrioxalate actinometry.

**Scheme 2**

as those obtained by CT activation (with identical molar ratios in Table 3).

To establish the photochemical efficiency of the quinone-activated cycloaddition, a 0.05 M solution of chloranil containing 0.01 M stilbene was irradiated with monochromatic light at  $\lambda_{exc} = 436$  nm, and quantitative measures of the light absorption were based on ferrioxalate actinometry.<sup>37</sup> The results in Table 3 show that the quantum efficiencies  $\Phi_Q$  exhibited the same trend with the substitution pattern of the stilbenes as those observed upon CT activation; that is, the highest efficiency ( $\Phi_Q = 0.48$ ) was obtained with the 4,4'-dichlorostilbene (7). Carbonyl activation resulted in a much more efficient formation of oxetane relative to the corresponding charge-transfer activation (compare columns 4 and 7 in Table 3). The difference can be explained by considering the spin multiplicities of the two reaction sequences in the following way.

Direct excitation of chloranil generates its triplet state with unit efficiency owing to the ultrafast rate of intersystem crossing.<sup>38</sup> The sizable energy of triplet quinone with  $E_T \approx 50$  kcal mol<sup>-1</sup><sup>39</sup> is sufficient to effect the ready oxidation of aromatic donors such as stilbenes at diffusion-limited rates<sup>40,41</sup> and to result in the formation of triplet ion-radical pairs (Scheme 2).

Triplet ion-radical pairs exhibit rather long lifetimes in comparison to the corresponding singlet ion pairs, since

(37) Hatchard, C. G.; Parker, C. A. *Proc. R. Soc.* **1956**, *235A*, 518. See also: Calvert, J. G.; Pitts, J. N., Jr. *Photochemistry*; Wiley: New York, 1996; p 786.

(38) (a) Rathore, R.; Hubig, S. M.; Kochi, J. K. *J. Am. Chem. Soc.* **1997**, *119*, 11468, and references therein. (b) Hubig, S. M.; Bockman, T. M.; Kochi, J. K. *J. Am. Chem. Soc.* **1997**, *119*, 2926.

(39) Murov, S. L.; Carmichael, I.; Hug, G. L. *Handbook of Photochemistry*, 2nd ed.; Dekker: New York, 1993.

(40) (a) Gschwind, R.; Haselbach, E. *Helv. Chim. Acta* **1979**, *62*, 941. (b) Johnson, L. J.; Schepp, N. P. *J. Am. Chem. Soc.* **1993**, *115*, 6564. (c) Levin, P. P.; Kuzmin, V. A. *Russ. Chem. Rev.* **1987**, *56*, 307.

(41) (a) Levin, P. P.; Kuzmin, V. A. *Bull. Russ. Acad. Div. Sci. Chem. Sci.* **1992**, *41*, 451. (b) Baciocchi, E.; Del Giacco, T.; Elisei, F.; Ioele, M. *J. Org. Chem.* **1995**, *60*, 7974.

back-electron transfer to the (*singlet*) ground-state represents a rather slow (spin-forbidden) process. As a consequence, the coupling process ( $k_C$ ) in Scheme 2 can better compete with the back-electron transfer and leads to the improved quantum efficiencies of oxetane formation in Table 3. In other words, the substantial difference in the quantum efficiencies of carbonyl-activated and CT-activated oxetane formation is readily accommodated by a mere consideration of the ion-pair spin multiplicities in an otherwise identical reaction sequence.

#### V. Direct Observation of Triplet Ion-Radical Pairs upon Laser Excitation of Chloranil in the Presence of Stilbene.

To directly observe the triplet ion-radical pairs as the result of electron-transfer quenching of triplet quinone, time-resolved absorption measurements were carried out on the picosecond and early nanosecond time scales as follows: A solution of chloranil (0.008 M) and stilbene (0.1 M) was excited with the 200 fs laser pulse of a Ti:sapphire laser tuned at 406 nm. At 50 ps after laser excitation, a transient spectrum was obtained which clearly showed the characteristic 510 nm absorption of triplet chloranil.<sup>38a,42</sup> This absorption decayed over a time span of about 1.5 ns, and the concomitant growth of the absorptions of chloranil anion radical<sup>21</sup> and stilbene cation radical<sup>20</sup> was observed at  $\lambda_{max} = 450$ , 480, and 760 nm (vide supra). Kinetics traces obtained at all three wavelengths could be fitted to first-order kinetics with a single rate constant of  $k = 2.5 \times 10^9$  s<sup>-1</sup>. The spectral changes were thus ascribed to the diffusional electron-transfer quenching of excited chloranil by stilbene with a second-order rate constant of  $k_q = k/[S] = 2.5 \times 10^{10}$  M<sup>-1</sup> s<sup>-1</sup>. In other words, triplet chloranil was quenched by stilbene at a diffusion-limited rate,<sup>43</sup> in accord with the highly exergonic electron transfer.<sup>44</sup> The resulting ion-radical absorptions subsequently decayed by first-order kinetics with a relatively long lifetime of  $\tau \approx 5$  ns, and they were thus assigned to the triplet ion-radical pair.

Let us now discuss the principal decay pathways of the triplet ion-radical pair shown in Scheme 2: Since ionic dissociation is disfavored in the nonpolar dioxane ( $k_{diss} \approx 0$ ), the decay of the ion pair can be entirely ascribed to back-electron transfer ( $k_{BET}$ ) or coupling ( $k_C$ ) which ultimately leads to the oxetane products. Thus, the competition between these predominant decay routes determines the quantum yields ( $\Phi_Q$ ) of oxetane formation

(42) On the early picosecond time scale, the singlet ion-radical pair is observed due to CT excitation of the chloranil/stilbene EDA complex, which also absorbed at 406 nm (vide supra).

(43) Diffusion-controlled reactions exhibit second-order rate constants of  $k \approx 10^{10}$  M<sup>-1</sup> s<sup>-1</sup>. See: Moore, J. W.; Pearson, R. G. *Kinetics and Mechanism*; Wiley: New York, 1981; p 239.

(44) Rehm, D.; Weller, A. *Isr. J. Chem.* **1970**, *8*, 259.

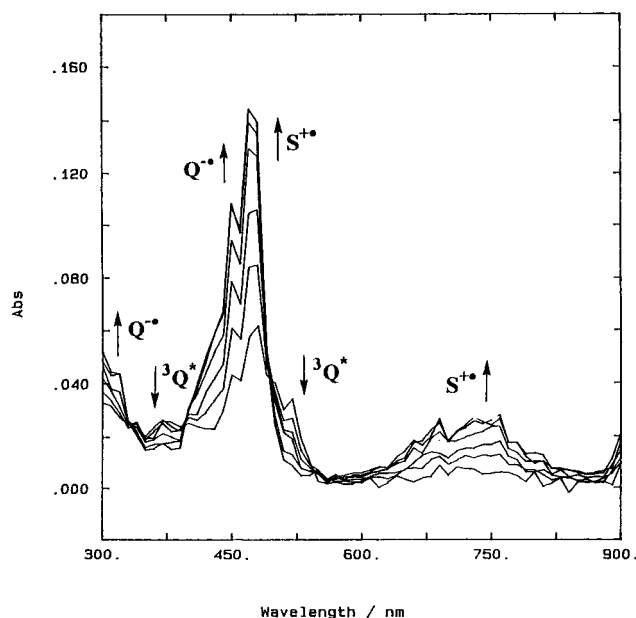


**Figure 4.** Spectral changes at 370, 430, 500, 620, 800, and 1000 ns following the application of a 10 ns laser pulse at  $\lambda_{\text{exc}} = 355$  nm to a solution of 0.0001 M stilbene and 0.004 M chloranil in acetonitrile.

in Table 3, i.e.,  $\Phi_Q = k_C/(k_C + k_{\text{BET}})$ . Accordingly, the (maximum) quantum yield of  $\Phi_Q = 0.48$  for stilbene **7** in dioxane is the result of about equal rates of back-electron transfer and coupling (i.e.,  $k_C \approx k_{\text{BET}} = 1 \times 10^8 \text{ s}^{-1}$ ) in the best case.

In a polar solvent such as acetonitrile, the diffusional quenching of excited chloranil (0.004 M) by stilbene (0.0001 M) also resulted in the formation of ion radicals as observed by time-resolved (ns/ $\mu\text{s}$ ) spectroscopy (see Figure 4). However, the ion radicals exhibited much longer ( $\mu\text{s}$ ) lifetimes as compared to those in dioxane, and they slowly decayed by second-order kinetics (not shown in Figure 4). We thus conclude that the ion radicals in acetonitrile are *not* ion-paired, but exist as free, solvated ions which recombine upon diffusional encounter on the  $\mu\text{s}$  time scale. The observation of free ion radicals in acetonitrile is due to efficient ion dissociation ( $k_{\text{diss}}$  in Scheme 2), which has been previously established to occur with rate constants of  $k_{\text{diss}} \approx 10^9 \text{ s}^{-1}$ .<sup>45,46</sup> Such fast ionic dissociation completely outruns the much slower (spin-forbidden) back electron transfer as revealed by the free-ion yields close to unity observed in acetonitrile,<sup>38a,40a</sup> and it also renders the rather slow coupling process ( $k_C$ ) completely suppressed ( $\Phi_Q = 0$ ) in acetonitrile.<sup>47</sup>

**VI. Mechanistic Implications of the Microdynamics for Singlet and Triplet Ion-Radical Pairs.** Time-resolved spectroscopy in two widely separated (ps and ns) time regimes establishes the singlet and triplet ion-radical pairs, i.e.,  $^1[\text{S}^{\bullet+}, \text{Q}^{\bullet-}]$  and  $^3[\text{S}^{\bullet+}, \text{Q}^{\bullet-}]$ , as the first intermediates in charge-transfer activation and carbonyl activation, respectively, of the stilbene/quinone pairs for the Paterno–Büchi photocycloadditions. Most strikingly, the quantitative analysis of the decay kinetics reveals

the microdynamics for ion-pair coupling to be rather independent of the spin state, with a relatively invariant value of  $k_C \sim 1 \times 10^8 \text{ s}^{-1}$  for *both* processes. As such, the difference between CT and carbonyl activation lies solely in the competitive rates of back electron transfer in singlet and triplet ion-radical pairs with  $k_{\text{BET}} = 3 \times 10^{11}$  and  $1 \times 10^8 \text{ s}^{-1}$ , respectively. Since the oxetane products are derived only as a result of ion-pair coupling, it follows from the identical values of  $k_C$  that carbonyl activation of the Paterno–Büchi reaction must proceed via an ion-radical pair that is essentially indistinguishable from that derived via photoinduced electron transfer within the intermolecular  $[\text{S}, \text{Q}]$  complex. It is noteworthy that such a conclusion (based on kinetics) coincides with that deduced from oxetane analysis (based on regioisomers)<sup>48</sup> to confirm the generality of the electron-transfer mechanism.<sup>23</sup>

## Summary and Conclusions

The Paterno–Büchi coupling of various stilbenes (**S**) with chloranil (**Q**) to yield *trans*-oxetane(s) is effectively achieved by the specific charge-transfer photoactivation of the electron donor–acceptor complexes  $[\text{S}, \text{Q}]$ . Time-resolved (ps) spectroscopy reveals the *singlet* ion-radical pair  $^1[\text{S}^{\bullet+}, \text{Q}^{\bullet-}]$  to be generated exclusively as the primary reactive intermediate and thus establishes its unambiguous role as the direct precursor of the oxetane and all the (coupled) intermediates.<sup>23</sup> Quantitative analysis of the singlet  $^1[\text{S}^{\bullet+}, \text{Q}^{\bullet-}]$  decay leads to  $k_C = 9 \times 10^7 \text{ s}^{-1}$  for ion-pair collapse to the 1,4-biradical  $^1\text{SQ}^{\bullet\bullet}$  and  $k_{\text{BET}} = 3 \times 10^{11} \text{ s}^{-1}$  for back electron transfer to regenerate the initial EDA complex. For comparison, carbonyl (quinone) activation (as usually employed in Paterno–Büchi couplings) leads to the same oxetane products (with identical isomer ratios). Thus, an analogous mechanism is applied which includes an initial electron-transfer quenching of the photoactivated (triplet) quinone acceptor by the stilbene donors resulting in *triplet* ion-radical pairs. Quantitative analysis of the triplet  $^3[\text{S}^{\bullet+}, \text{Q}^{\bullet-}]$  decay leads to  $k_C = 1 \times 10^8 \text{ s}^{-1}$  for ion-pair collapse to the biradical and  $k_{\text{BET}} = 1 \times 10^8 \text{ s}^{-1}$  for the (spin-forbidden) back electron transfer. The substantial differences in the quantum efficiencies of CT-activated versus carbonyl-activated oxetane formation are thus readily explained by a simple consideration of the difference in the spin multiplicity (i.e., singlet versus triplet) in the ion-radical pairs in otherwise identical mechanisms of ion-pair microdynamics. As such, the electron-transfer mechanism established here (for the first time) for a typical Paterno–Büchi coupling of chloranil and stilbene forms the basis for the quantitative evaluation of various solvent and salt effects, which will be reported separately.<sup>47</sup>

## Experimental Section

**Materials and Methods.** Chloranil was sublimed in vacuo and recrystallized from benzene. (*E*)-stilbene from Aldrich was used as received. The chloro- and methyl-substituted stilbenes **2–8** were prepared via the Wittig coupling of the correspond-

(45) Knibbe, H.; Rehm, D.; Weller, A. *Ber. Bunsen-Ges. Phys. Chem.* **1968**, *72*, 257.

(46) Ojima, S.; Miyasaka, H.; Mataga, N. *J. Phys. Chem.* **1990**, *94*, 7534.

(47) A detailed study of the solvent effects on the back electron transfer, the ion dissociation, and the coupling processes will be published later.

(48) Regiochemistry in the electron-transfer mechanism<sup>23</sup> is determined by the relative orientation of the ion-radical pair, particularly as it is affected by the *charge* distribution. [As such, the spin multiplicity of the singlet or triplet biradical state does not appear to be a distinguishing factor.] Charge annihilation in the triplet ion-radical pair may proceed either directly to the 1,4-biradical or via spin inversion followed by ion-pair collapse to the singlet 1,4-biradical.



ing ylides and aldehydes.<sup>49</sup> The *trans* isomers were isolated by flash chromatography, and HPLC analyses showed that they were not contaminated by the other (*cis*) isomers. Acetonitrile and dioxane were purified according to published procedures.<sup>50</sup> Melting points are uncorrected. <sup>1</sup>H NMR and <sup>13</sup>C NMR were recorded in CDCl<sub>3</sub> on a 300 MHz NMR spectrometer. UV-vis absorption and infrared spectra were recorded on a diode-array spectrometer and a Fourier transform spectrometer, respectively. GC-MS analyses were carried out on gas chromatograph interfaced to a mass spectrometer (EI, 70 eV). HPLC analyses were performed using a Hypersil BDS C18 reverse-phase column (20 cm) with methanol/water mixtures as eluent. All chemical analyses were carried out by Atlantic Microlab Inc., Norcross, GA. The oxidation (peak) potentials of the *trans*-stilbenes were determined by cyclic voltammetry.

**Photoinduced Coupling of Chloranil with Stilbenes. General Procedure for the Preparative Photolysis.** A solution of chloranil (1 mmol, 0.05 M) and stilbene<sup>51</sup> (2 mmol, 0.1 M) in benzene was prepared under an argon atmosphere and irradiated with a focused beam from a medium-pressure mercury lamp (500 W) passed through an aqueous IR filter and a 370 nm sharp cutoff filter. This ensured that only the quinone (and not the stilbene) absorbed the actinic light. The photoreaction was carried out until periodic HPLC analysis showed that all chloranil was consumed. The solvent was evaporated, and in the case of unsymmetrical stilbenes, the relative ratio of the two regioisomers of spirooxetanes was determined by <sup>1</sup>H NMR.<sup>31</sup> For example, the chemical shift of the  $\alpha$  proton in **6A** ( $\delta$  6.58) was slightly shifted upfield as compared to that in isomer **6B** ( $\delta$  6.63), and the  $\beta$  proton in **6A** was slightly shifted downfield ( $\delta$  4.96) compared to the isomer **6B** ( $\delta$  4.83), as confirmed in the X-ray structure analyses. The crude product was washed with petroleum ether and recrystallized from chloroform/petroleum ether. The spirooxetane (containing two regioisomers for the unsymmetrical stilbenes) was isolated in high yield (81–87%) based on the chloranil conversion. All attempts to separate the regioisomers by preparative TLC (alumina or silica gel) with numerous solvent combinations and ratios (including ethyl acetate, ethyl ether, dichloromethane, hexane, benzene, and petroleum ether) remained unsuccessful. However, some of the isomers (**2A**, **3B**, **5B**, and **6B**) could be separated from the isomeric mixture by stepwise crystallization from chloroform/petroleum ether, and the structures of **2A**, **3B**, and **6B** were established by X-ray crystallography.<sup>52</sup> Characteristic physical data for the spirooxetane products are as follows:

**5,6,8,9-Tetrachloro-2,3-diphenyl-1-oxaspiro[3,5]nona-5,8-dien-7-one, 1A:** mp 150–151 °C (decomp) (lit. 150 °C);<sup>24</sup> IR (cm<sup>-1</sup>) 1686, 1606, 1575, 1497, 1127, 1102, 968, 826, 773, 753, 742, 733, 723, 698, 682, 651, 551; <sup>1</sup>H NMR (CDCl<sub>3</sub>)  $\delta$  4.98 (d, 1H, J 8.7), 6.72 (d, 1H, J 9.0), 7.30–7.60 (m, 10H).

**5,6,8,9-Tetrachloro-2-(4-chlorophenyl)-3-phenyl-1-oxaspiro[3,5]nona-5,8-dien-7-one, 2A:** mp 143–144 °C (lit. 144–146 °C);<sup>24</sup> IR (cm<sup>-1</sup>) 1671, 1600, 1570, 1490, 1279, 1120, 1101, 982, 956, 810, 784, 735, 724, 690, 682, 650, 553; <sup>1</sup>H NMR (CDCl<sub>3</sub>)  $\delta$  4.95 (d, 1H, J 8.7), 6.68 (d, 1H, J 8.7), 7.27–7.58 (m, 9H).

**5,6,8,9-Tetrachloro-2-phenyl-3-(4-chlorophenyl)-1-oxaspiro[3,5]nona-5,8-dien-7-one, 2B:** Could not be fully separated from isomer **2A**; <sup>1</sup>H NMR (CDCl<sub>3</sub>)  $\delta$  4.93 (d, 1H, J 8.7), 6.66 (d, 1H, J 8.7), 7.27–7.58 (m, 9H).

**5,6,8,9-Tetrachloro-2-(3,4-dichlorophenyl)-3-phenyl-1-oxaspiro[3,5]nona-5,8-dien-7-one, 3A:** Could not be fully

separated from isomer **3B**; <sup>1</sup>H NMR (CDCl<sub>3</sub>)  $\delta$  4.96 (d, 1H, J 9.0), 6.63 (d, 1H, J 8.7), 7.39–7.65 (m, 8H).

**5,6,8,9-Tetrachloro-2-(3,4-dichlorophenyl)-3-phenyl-1-oxaspiro[3,5]nona-5,8-dien-7-one, 3B:** mp 155–157 °C (decomp); IR (cm<sup>-1</sup>) 1676, 1608, 1573, 1497, 1476, 1447, 1407, 1283, 1220, 1144, 1120, 1099, 1035, 980, 959, 919, 896, 872, 851, 835, 822, 780, 759, 743, 730, 714, 698, 679, 650, 598, 579, 561, 537, 476, 460, 445; <sup>1</sup>H NMR (CDCl<sub>3</sub>)  $\delta$  4.92 (d, 1H, J 9.0), 6.66 (d, 1H, J 9.0), 7.39–7.65 (m, 8H). Anal. Calcd for C<sub>20</sub>H<sub>10</sub>Cl<sub>6</sub>O<sub>2</sub>: C, 48.51; H, 2.02. Found: C, 48.41; H, 2.01.

**5,6,8,9-Tetrachloro-2-(4-methylphenyl)-3-phenyl-1-oxaspiro[3,5]nona-5,8-dien-7-one, 4A:** Could not be fully separated from isomer **4B**; <sup>1</sup>H NMR (CDCl<sub>3</sub>)  $\delta$  2.41 (s, 3H), 5.02 (d, 1H, J 9.0), 6.71 (d, 1H, J 8.7), 7.00–7.60 (m, 9H).

**5,6,8,9-Tetrachloro-2-(3,4-dichlorophenyl)-3-phenyl-1-oxaspiro[3,5]nona-5,8-dien-7-one, 4B:** Could not be fully separated from isomer **4A**; <sup>1</sup>H NMR (CDCl<sub>3</sub>)  $\delta$  2.36 (s, 3H), 4.95 (d, 1H, J 9.0), 6.73 (d, 1H, J 8.7), 7.00–7.60 (m, 9H).

**5,6,8,9-Tetrachloro-2-(4-methylphenyl)-3-(4-chlorophenyl)-1-oxaspiro[3,5]nona-5,8-dien-7-one, 5A:** Could not be fully separated from isomer **5B**; <sup>1</sup>H NMR (CDCl<sub>3</sub>)  $\delta$  2.42 (s, 3H), 4.97 (d, 1H, J 9.0), 6.68, 2.42 (s, 3H), 4.97 (d, 1H, J 9.0), 6.68 (d, 1H, J 8.7), 6.99–7.52 (m, 8H).

**5,6,8,9-Tetrachloro-2-(4-chlorophenyl)-3-(4-methylphenyl)-1-oxaspiro[3,5]nona-5,8-dien-7-one, 5B:** mp 132–134 °C (decomp); IR (cm<sup>-1</sup>) 1675, 1601, 1570, 1493, 1448, 1408, 1302, 1286, 1217, 1142, 1118, 1089, 1034, 980, 958, 917, 895, 871, 854, 834, 812, 780, 759, 744, 730, 714, 697, 679, 649, 597, 579, 561, 536, 476, 461, 454; <sup>1</sup>H NMR (CDCl<sub>3</sub>)  $\delta$  2.36 (s, 3H), 4.89 (d, 1H, J 9.0), 6.67 (d, 1H, J 8.7), 6.99–7.52 (m, 8H). Anal. Calcd for C<sub>21</sub>H<sub>13</sub>Cl<sub>5</sub>O<sub>2</sub>: C, 53.14; H, 2.74. Found: C, 53.14; H, 2.83.

**5,6,8,9-Tetrachloro-2-(4-methylphenyl)-3-(3,4-dichlorophenyl)-1-oxaspiro[3,5]nona-5,8-dien-7-one, 6A:** Could not be fully separated from isomer **6B**; <sup>1</sup>H NMR (CDCl<sub>3</sub>)  $\delta$  2.40 (s, 3H), 4.96 (d, 1H, J 8.7), 6.58 (d, 1H, J 9.0), 6.92–7.61 (m, 7H).

**5,6,8,9-Tetrachloro-2-(3,4-dichlorophenyl)-3-(4-methylphenyl)-1-oxaspiro[3,5]nona-5,8-dien-7-one, 6B:** mp 141–143 °C (decomp); IR (cm<sup>-1</sup>) 1674, 1601, 1571, 1493, 1449, 1407, 1301, 1216, 1140, 1119, 1088, 978, 960, 918, 896, 871, 780, 759, 742, 730, 697, 678, 649, 596, 578, 561, 536, 476, 461; <sup>1</sup>H NMR (CDCl<sub>3</sub>)  $\delta$  2.34 (s, 3H), 4.83 (d, 1H, J 7.8), 6.63 (d, 1H, J 8.1), 7.30–7.60 (m, 7H). Anal. Calcd for C<sub>21</sub>H<sub>12</sub>Cl<sub>6</sub>O<sub>2</sub>: C, 49.54; H, 2.36. Found: C, 49.52; H, 2.41.

**5,6,8,9-Tetrachloro-2-(4-chlorophenyl)-3-(4-chlorophenyl)-1-oxaspiro[3,5]nona-5,8-dien-7-one, 7A:** mp 162–164 °C (decomp); IR (cm<sup>-1</sup>): 1682, 1603, 1568, 1494, 1119, 1106, 1100, 1012, 971, 955, 941, 914, 884, 829, 758, 745, 731, 523; <sup>1</sup>H NMR (CDCl<sub>3</sub>)  $\delta$  4.91 (d, 1H, J 8.7), 6.65 (d, 1H, J 8.7), 7.04 (d, 2H, J 8.4), 7.37 (d, 2H, J 8.7), 7.43–7.57 (m, 4H). Anal. Calcd for C<sub>20</sub>H<sub>10</sub>Cl<sub>6</sub>O<sub>2</sub>: C, 48.51; H, 2.02. Found: C, 48.57; H, 2.05.

**5,6,8,9-Tetrachloro-2-(3,4-dichlorophenyl)-3-(3,4-dichlorophenyl)-1-oxaspiro[3,5]nona-5,8-dien-7-one, 8A:** mp 169–171 °C (decomp); IR (cm<sup>-1</sup>) 1690, 1575, 1475, 1449, 1386, 1363, 1127, 1103, 1028, 983, 974, 8221, 769, 754, 733, 666, 650, 542; <sup>1</sup>H NMR (CDCl<sub>3</sub>)  $\delta$  4.88 (d, 1H, J 8.7), 6.57 (d, 1H, J 8.7), 6.87 (d, 1H, J 8.4), 7.34–7.38 (m, 2H), 7.47 (d, 1H, J 8.4), 7.56 (d, 1H, J 8.4), 7.62 (d, 1H, J 1.8). Anal. Calcd for C<sub>20</sub>H<sub>8</sub>Cl<sub>8</sub>O<sub>2</sub>: C, 42.58; H, 1.42. Found: C, 42.51; H, 1.47.

**Quantum Yield for the Photocoupling of Chloranil with Stilbenes. Excitation at  $\lambda_{exc} > 480$  nm.** The quantum yields were measured with the aid of a medium-pressure (500 W) mercury lamp focused through an aqueous IR filter followed by a 480 nm cutoff filter. The intensity of the lamp was determined with a freshly prepared potassium reineckate solution.<sup>34</sup> Equimolar (0.1 M) solutions of chloranil and (*E*)-stilbene were irradiated, and the photoconversion was monitored by HPLC. The product formation was quantified with biphenyl as internal standard. Since the actinic light was not completely absorbed by the reaction mixture, a correction for transmitted light was made.

**Excitation at  $\lambda_{exc} = 436$  nm.** The quantum yields were measured with the same lamp focused through an aqueous

(49) McDonald, R. N.; Campbell, T. W. In *Organic Syntheses*; Wiley: New York, 1973; Vol. 5; p 499.

(50) Perrin, D. D.; Armarego, W. L. F.; Perrin, D. R. *Purification of Laboratory Chemicals*, 2nd ed.; Pergamon: New York, 1980.

(51) Since (*Z*)- and (*E*)-isomers generally yield the same spirooxetane(s),<sup>24</sup> the isomeric mixture (*E:Z* 65–70:30–35) of the stilbenes was used for preparative photocouplings. Quantum yields are determined with pure (*E*)-isomers as starting materials, and the photoreactivity of (*Z*)-stilbene is described separately.<sup>47</sup>

(52) On deposit with the Cambridge Crystallographic Data Center, 12 Union Road, Cambridge, CB12 1EZ, U.K.



IR filter followed by an aqueous  $\text{NaNO}_2/\text{CuSO}_4$  solution filter with a narrow-band-pass at  $440 \pm 30$  nm. The intensity of the lamp was determined with a freshly prepared potassium ferrioxalate actinometer solution.<sup>37</sup> The absorbance at 436 nm of the solutions of chloranil (0.05 M) and (*E*)-stilbenes (0.1 M) in dioxane remained above 1.5 throughout the irradiation, and thus no correction for transmitted light was necessary.

**Charge-Transfer Absorption Spectra of EDA Complexes of Chloranil with Stilbene Donors. Benesi–Hildebrand Evaluation.** The vivid colors that were observed upon addition of stilbenes to a chloranil solution persisted indefinitely when the solutions were kept in the dark, and most importantly, the components **S** and **Q** could be quantitatively recovered intact from mixtures that were stored for several days at room temperature in the dark. The UV–vis spectral changes shown in Figure 1 demonstrate that the colored solutions resulted from a new (additional) absorption band with  $\lambda_{\text{max}} \approx 510$  nm, the intensity of which increased with incremental additions of stilbene. Such color changes are diagnostic of the preequilibrium formation of electron donor–acceptor (EDA) complexes (see eq 2),<sup>15,16</sup> and they are ascribed to charge-transfer absorptions. The absorbance changes ( $A_{\text{CT}}$ ) were monitored at the absorption maximum ( $\lambda_{\text{CT}}$ ) and quantitatively evaluated with the aid of the Benesi–Hildebrand relationship.<sup>29</sup> Thus a benzene solution of 0.005 M chloranil was prepared in a quartz cuvette, and the UV–vis absorption spectrum of the yellow solution was recorded. Stilbene (44.9 mg, 0.0831 M) was added and the absorption spectrum re-recorded. The absorption spectrum of chloranil was digitally subtracted and the difference hereinafter referred to as the charge-transfer (CT) absorption spectrum (see inset in Figure 1). To determine the formation constant of the CT complex, the concentrations of chloranil and stilbene donors were chosen such that the stilbene was added incrementally in large excess (i.e.,  $[\mathbf{Q}] = 0.005$  M and  $[\text{stilbene}]$  ranging from 0.0242 to 0.0831 M). The charge-transfer absorptions at the spectral maxima ( $A_{\text{CT}}$ ) were determined and quantitatively evaluated applying the Benesi–Hildebrand relationship,<sup>29</sup> i.e.,

$$\frac{[\mathbf{Q}]}{A_{\text{CT}}} = \frac{1}{K_{\text{EDA}}\epsilon_{\text{CT}}[\mathbf{S}]} + \frac{1}{\epsilon_{\text{CT}}} \quad (7)$$

where  $K_{\text{EDA}}$  represents the formation constant and  $\epsilon_{\text{CT}}$  the extinction coefficient of the EDA complex. The values of  $K_{\text{EDA}}$  and  $\epsilon_{\text{CT}}$  extracted from the linear correlation of  $[\mathbf{Q}]/A_{\text{CT}}$  versus  $[\mathbf{S}]^{-1}$  are reported in Table 1 together with the absorption maxima of the EDA complexes. The absorption maxima  $\lambda_{\text{CT}}$  of the EDA complexes were directly related to the donor strength of the various (*E*)-stilbenes evaluated by their anodic peak potentials ( $E_{\text{ox}}^{\text{p}}$ ) (see Table 1), and thus the progressive blue shift of the absorption band for chloro substitution and red shift for methyl substitution confirm the charge-transfer character of the EDA complex in eq 2 according to Mulliken theory.<sup>32</sup>

**Time-Resolved Absorption Spectroscopy. Direct Excitation of Chloranil at  $\lambda_{\text{exc}} = 355$  nm.** The nanosecond

time-resolved absorption measurements were carried out with a kinetic spectrometer including a Q-switched  $\text{Nd}^{3+}$ :YAG laser (10 ns pulse width).<sup>53</sup> The third (355 nm) harmonic output was used for the excitation of chloranil. The solutions of chloranil and (*E*)-stilbenes were prepared under an argon atmosphere in a 1 cm cuvette fitted with a Schlenk adapter. The concentrations of the components were adjusted for absorbances in the range 0.5–0.8 at the excitation wavelength of  $\lambda_{\text{exc}} = 355$  nm.

**Charge-Transfer Excitation at  $\lambda_{\text{exc}} = 532$  nm.** The picosecond transient absorption measurements following charge-transfer excitation of the EDA complex between chloranil and stilbene were performed with a mode-locked  $\text{Nd}^{3+}$ :YAG laser using the second-harmonic output at 532 nm (17 mJ per pulse).<sup>53</sup>

**Laser Excitation at 406 nm.** To monitor the quenching of photoexcited quinone by stilbene in dioxane on the picosecond time scale, chloranil was excited at 406 nm (to avoid the unintentional photoexcitation of stilbene). The excitation at 406 nm was achieved with a Ti:sapphire laser system consisting of a Ti:sapphire oscillator coupled to an argon-ion laser and two consecutive Ti:sapphire amplifiers pumped by a Nd:YAG laser at 10 Hz.<sup>54</sup>

**Electrochemical Measurements.** The cyclic voltammetry (CV) measurements were carried out with a cell that was of an airtight design with high-vacuum Teflon valves and Viton O-ring seals to allow an inert atmosphere to be maintained without contamination by grease. The working electrode consisted of an adjustable platinum disk embedded in a glass seal to allow periodic polishing (with a fine emery cloth) without changing the surface area (of about 1 mm<sup>2</sup>) significantly. The SCE reference electrode and the associated salt bridge were separated from the catholyte by a sintered glass frit. The counter electrode consisted of a platinum gauze that was placed about 3 mm from the working electrode. The CV measurements were carried out under an argon atmosphere with 5 mM stilbene in dry acetonitrile containing 0.1 M tetra-*n*-butylammonium hexafluorophosphate as supporting electrolyte. All cyclic voltammograms were recorded at sweep rates of 100 mV s<sup>-1</sup> and were *iR* compensated. The oxidation (peak) potentials of the stilbenes in Chart 1 were referenced to SCE, which was calibrated with ferrocene (5 mM) as the internal standard.

**Acknowledgment.** We thank S. V. Lindeman for crystallographic assistance, and the National Science Foundation and the Robert A. Welch Foundation for financial support.

JO981754N

(53) Bockman, T. M.; Kochi, J. K. *J. Chem. Soc., Perkin Trans. 2* **1996**, 1633.

(54) Hubig, S. M.; Bockman, T. M.; Kochi, J. K. *J. Am. Chem. Soc.* **1996**, *118*, 3842.